University of Thi-Qar Journal for Engineering Sciences
Volume 15, Issue 1, June 2025
https://doi.org/10.31663/utjes.15.1.698

Modeling and design procedure for LiBr-water absorption air-conditioning by solar energy

Sanaa M . Hadi [1], Mushtaq I. Hasan [1]

Received: 29th December 2024/Accepted: 7th March 2025/ Published Online: 1st June 2025

Abstract

The aim of this study is to design a lithium bromide-water (LiBr-H2O) absorption cooling system with a rated capacity of about 1 kW of solar-powered cooling using lithium bromide as an adsorbent and water as a refrigerant. The proposed absorption cooling system consists of a rooftop evacuated tube solar collector, a LiBr-H2O single-effect absorption chiller (including a generator, a solution heat exchanger, an evaporator, a condenser, and an absorber), a fan coil unit, pumps, a flow choke, and control valves. All the governing thermal equations of the system were studied theoretically, and the system was designed according to the following assumptions (system capacity 1 kW, generator temperature 85℃, condenser temperature 38℃, evaporator temperature 5℃, and absorber temperature 37℃ing. To find out how different operational and design factors affect the thermal efficiency, a thermodynamic analysis of the absorption cooling cycle was performed. The dimensions of the components and the cooling capacity were explored in the results.

Keywords—Lithium Bromide–Water, Solar-Powered Cooling, Thermodynamic Analysis, Refrigeration Cycle, Heat Exchanger Design, Sustainable Cooling Systems.

1 Introduction

The utilization of solar energy in Refrigeration and Air Conditioning applications is on the rise, contributing to the decrease in the use of fossil fuels and the mitigation of greenhouse gas emissions. Traditional air conditioning systems rely on electricity for their functioning. The imperative requirement of recent times is the adoption of environmentally sustainable and energy-efficient technologies to supplant traditional refrigeration and air conditioning systems. A solar-assisted absorption air conditioning system is thought to be a practical way to meet a building's heating and cooling requirements (Eicker & Pietruschka, 2009). Currently, a comfortable and healthy environment is widely recognized as essential, and numerous contemporary procedures and goods rely heavily on the accurate management of environmental factors. This underscores the proliferation of computer programs in the realm of air conditioning aimed at establishing the most suitable building layout that ensures human comfort in terms

Sanaa M . Hadi[1]
Sana.m@utq.edu.iq
Mushtaq I. Hasan[1]
mushtaq@utq.edu.iq

[1] Mechanical Engineering Department, College of Engineering, University of Thi-Qar, Thi-Qar, Iraq

of temperature while minimizing energy consumption. Potential replacements for commercial air conditioning systems that use water and lithium bromide. The way absorption chillers work is by taking heat from the interior air and transferring it to lithium bromide and a water-based solution. The heat is then released outside by heating this mixture. Rather than applying electricity, a heat source powers this system.

There are many researchers in the literature who have studied the absorption system, such as Eicker, U., and Pietruschka, D. (2009) (Osman & Abdalla, 2016), who studied the contribution to solar thermal absorption chiller system design. For absorption cooling systems, a comprehensive simulation model was created together with a stratified storage tank, a steady-state or dynamic collector model, and hourly lyre solved building loads. Using experimental data from many solar cooling facilities, the model was validated. The control method has a significant impact on the design and performance of the solar thermal system since, under partial load situations, the absorption chillers may run at lower generating temperatures. KETFI, Omar, et al (2015) (Ketfi et al., 2015) studied a single-stage absorption refrigeration system with LiBr-H2O. Results were compared to another mathematical model. COP increases with higher evaporator and generator temperatures, but decreases with higher condenser and absorber temperatures. The system's maximum COP was 0.77 at a generator temperature of 92°C, close to the manufacturer's value. Narayanan, R. et al (2021) (Narayanan et al., 2021) examined the potential of utilizing solar absorption cooling technology in student residence buildings in the subtropical climate of Australia, showing that maintaining room temperature between 20 and 24 ◦C with a solar absorption chiller can provide comfort. Optimization experiments indicated that a high solar fraction (SF) of 0.91 is achievable with a collector area of 20 m^2 and a storage ratio of 0.02 $\mathrm{m}^3/\mathrm{m}^2$ was achieved, while economic analysis was conducted to determine the payback period, annual energy cost savings, and carbon emission reduction. Ljuhani, Y. et al. (2022) (Aljuhani & Dayem, 2022) conducted a simulated investigation using TRNSYS to examine the potential of solar cooling with thermal energy storage for a hypothetical tent located in the Mina region of Saudi Arabia. The findings of this study indicated that to maintain the air temperature within the zone at (24 ◦C) for a duration of seven days in the summer period, an estimated cooling capacity of approximately (70 kW) (equivalent to 20 tons of refrigeration) is required.

In this paper an absorption LiBr-water system powered by solar energy has been anal with focusing on design procedure and thermodynamic analysis in the city of Nasiriyah, southern Iraq, at longitude (46.22) and latitude (31.13).

2 Components of a Solar Absorption Cooling System

The required cooling capacity and the thermodynamic characteristics of the working fluid pair determine the size and the various system components. Figure 1 shows the parts of the solar absorption cooling system.

3 Absorption System Design

The thermodynamic design of lithium bromide – water. According to the first law of thermodynamics, an absorption cooling system operates under steady-state conditions. For the system point shown in Figure 1.

The presented design in this paper is for a LiBr-water absorption cooling cycle having a refrigerating capacity of 1 kW. A condenser temperature of 38°C, an absorber temperature of 37°C, and a Generator temperature 85 ℃ and evaporator temperature is 5℃ are selected. For the evaporator at temperatures 5℃from the steam table, the pressure is equal to 0.872 kPa, assuming the difference between the evaporator and absorber pressure 0.133 $kpas$ (Dalichaouch, 1989). For the equilibrium chart for LiBr solution at temperature of absorber 37 ℃, at a pressure of 0.7395 kPa, the concentration of the strong solution is $59\ \%$. From the steam table saturation pressure of water vapor in the condenser at a temperature of 38 ℃, and a pressure of 6.632 kpa, assuming the difference between the condenser pressure and the generator pressure is 3% (Dalichaouch, 1989), the pressure of the generator becomes 6.8309 kpa. For the equilibrium chart for LiBr solution, the concentration of the weak solution is 60 %.

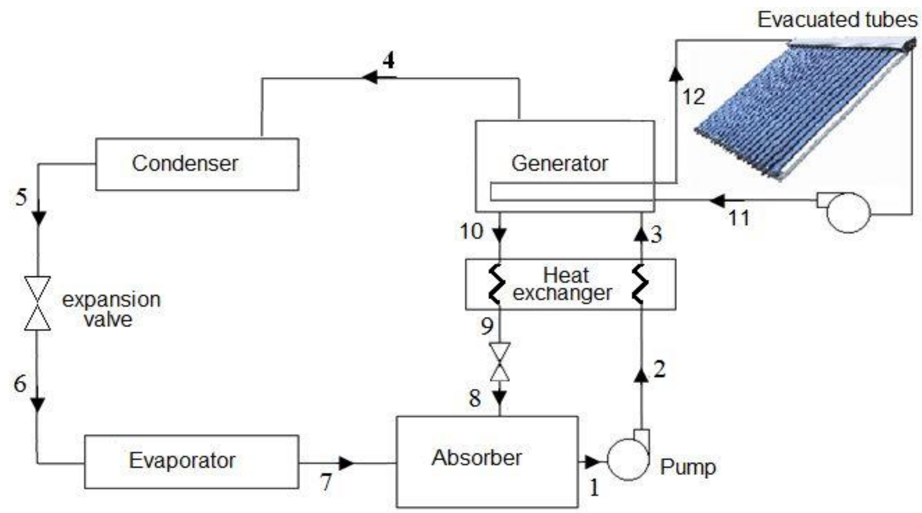

Figure 1: schematic representation of a solar absorption cooling system component (Ataa & Ammarib, n.d.)

3.1 Thermodynamic Analysis of the System Based on Mass and Energy Balance

Every cycle component's mass and energy balance under steady state conditions forms the basis of the simulation.

Assume the effectiveness of heat exchanger is 50% in this design (William et al., 2017)

$$E = \frac{(T_G - T_5)}{(T_G - T_a)} \quad \rightarrow T_5 = 61, \tag{1}$$

where

T_5 : Temperature of the weak solution leaving heat exchanger to absorber.

$$T_3 = T_a + \left[E * \left(\frac{X_{ws}}{X_{ss}}\right) * \left(\frac{C_{ss}}{C_{ws}}\right) * (T_G - T_a)\right], \tag{2}$$

where

T_3: Temperature of the strong solution leaving heat exchanger to generator.

C_{ss}: specific heat of strong solution calculated by using following relation:

$$C_{ss} = 4.184 * \left(1.01 - 1.23\, X_{ss} + 0.48\, {X_{ss}}^2 \right) \tag{3}$$

C_{ws}: specific heat of weak solution can calculated by using following relation:

$$C_{ws}: 4.184 * \left(1.01 - 1.23\, X_{ws} + 0.48\, {X_{ws}}^2\right) \tag{4}$$

$\therefore\ T_3 = 57.9℃$

The mass flow rate for weak and strong solution:

$\dot{m}_1 = \dot{m}_2 = \dot{m}_3 = \dot{m}_{ss}$

$\dot{m}_4 = \dot{m}_5 = \dot{m}_6 = \dot{m}_{ws}$

$\dot{m}_7 = \dot{m}_8 = \dot{m}_9 = \dot{m}_r$

The rate of heat transfer to the evaporator:

$$\dot{Q}_E = \dot{m}_r\,(h_{10} - h_9) \quad \rightarrow \quad \dot{m}_r = \frac{Q_E}{(h_{10} - h_9)}, \tag{5}$$

$$\therefore\ \dot{m}_r = 4.253 * 10^{-4}\ kg/s$$

The mass balance for solution:

$$\dot{m}_{ss} X_{ss} = \dot{m}_{ws}\, X_{ws} \tag{6}$$

From overall mass balance:

$$\dot{m}_{ss} = \dot{m}_{ws} + \dot{m}_r \tag{7}$$

$$\therefore\ m_{ss} = 0.01501\ kg/s, \quad m_{ws} = 0.0145\ kg/s$$

The rate of heat transfer from the absorber is

$$\dot{Q}_a = m_{ws} h_6 + m_r h_{10} - m_{ss} h_1 \tag{8}$$

The rate of heat transfer from the condenser is

$$Q_C = m_r (h_7 - h_8) \tag{9}$$

The rate of heat transfer from the generator is

$$Q_g = m_{ws} h_4 + m_r h_7 - m_{ss} h_3 \tag{10}$$

The rate of heat transfer from the heat exchangers

$$Q_H = m_{ss}(h_3 - h_2) = m_{ws}(h_4 - h_5) \tag{11}$$

where

$$h_1 = h_2 = enthalpy\ at\ (T_1 = T_a, X_{ss})$$

$$h_3 = enthalpy\ at\ (T_3, X_{ss})$$

$$h_4 = enthalpy\ \ at\ (T_4 = T_7 = T_G, X_{ws})$$

$$h_5 = h_6 = enthalpy\ \ at\ (T = T_5, X_{ws}) \qquad * throttling\ proccess$$

$$h_7 = enthalpy\ (T_7 = T_G)$$

$$h_8 = h_9 = enthalpy\ at\ (T_8 = T_C) \qquad * throttling\ proccess$$

$$h_{10} = enthalpy\ at\ (T_{10} = T_E)$$

The heat flow in the generator, absorber and condenser are calculated as:-

$$Q_G = 2.2\ kw$$

$$Q_a = 2.5\ kw$$

$$Q_C = 0.909\ kw$$

$$Q_E = 1\ kw$$

$$Q_H = 1.08\ kw$$

3.2 Calculation of Generator parameters

The absorption cooling system's generating unit typically has a submerged shell and coil design, with the hot water-carrying coil submerged in the cycle working fluid solution. The mass balance and energy balance for Generator shown in Figure 2. And the generator conditions are listed in Table 1. Table 2 include the properties of fluids in cycle.

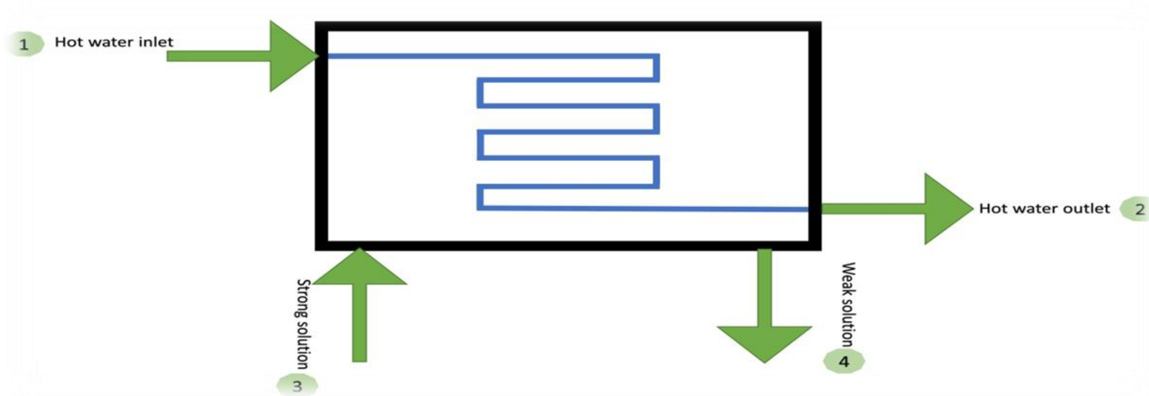

Figure 2: The mass balance and energy balance for the Generator

Table 1: Inlet and outlet data to the Generator

$\dot{Q}_g$	T_g	T_{ss}	$\dot{m}_{ss}$	X_{ss}	T_{ws}	$\dot{m}_{ws}$	X_{ws}	$T_{hw,i}$	$T_{hw,e}$	T_{av}
2.2	85	57.9	0.01501	59	85	0.0145	60.7	88	86	87
Kw	℃	℃	kg/s	%	℃	kg/s	%	℃	℃	℃

Table 2: the properties of hot water and the properties of LiBr-water (Klein & Alvarado, 2004)

The properties of hot water at mean temperature T=87 ℃			The properties of LiBr-water solution at T=71.6 ℃ and $\overline{X}$ = 59.9%		
ρ_w	966.7	kg/m^3	ρ	1689	kg/m^3
μ_w	0.000327	$kg/m.s$	μ	0.003061	$kg/m.s$
k_w	0.675	$w/m.c$	K	0.4434	$w/m.c$
C_{Pw}	4.199	$kJ/kg.c$	C_p	1.941	$KJ/kg.c$

First, the hot water flow within the coil's inner heat transfer coefficient (hi) is calculated, the mass flow rate of hot water is:

$$\dot{m}_w = \frac{\dot{Q}_G}{C_{p,w}\,\Delta t_w} = 0.524\ kg/s \quad (12)$$

The inside diameter of tubes is assumed D_{inner} = 0.014 m

The outside diameter of tube is assumed D_o = 0.016 m

The Reynolds number determines as

$$R_e = \frac{\dot{m}_w\ D_i}{A\ \mu} = \frac{4\ \dot{m}_w}{\pi\mu\ D_i} = 14580.9 \text{ (flow is turbulent).} \quad (13)$$

$$Nu = 0.023{R_e}^{0.8}\,Pr^n \quad (14)$$

n=0.4 for heating, n = 0.3 for cooling [10]
$\therefore$ n = 0.3 $\rightarrow$ Nu = 60.954
Nu = $\frac{D_\circ\ h_i}{K}$ $\rightarrow$ $h_i = \frac{Nu * k}{D_i} = 2938.9\ \frac{W}{m^2 °C}$ (15)
The outside heat transfer cofficent is evuluted from the following conditions:
For $\frac{4\,\Gamma}{\mu} < 2100$

$$\therefore h_\circ = 0.50\left[\frac{m^2\ \rho^{4/3}\ \ c_p\ g^{2/3}}{\frac{\pi\ \ D_\circ}{2}\ \left(\mu^{1/3}\right)}\right][\frac{\mu}{\mu_{wall}}]^{1/4}\ [\frac{4\,\Gamma}{\mu}]^{\frac{1}{9}} \quad (16)$$

For $\frac{4\Gamma}{\mu} > 2100$

$$h_\circ = 0.01\left[\frac{k^3\ \rho^2\ g}{\mu^2}\right]^{1/3}\left[\frac{\mu\ C_p}{k}\right]^{1/3}[\frac{4\,\Gamma}{\mu}]^{1/3} \quad (17)$$

In this design

$$\Gamma = \frac{\dot{m_{ws}}}{2\ L_{tube}} = 0.0242 \quad (18)$$

$$\frac{4\Gamma}{\mu} = 31.6 < 2100$$

$$h_\circ = 0.50\left[\frac{k^2\ \rho^{4/3}\ c_p\ g^{2/3}}{\frac{\pi\ D_\circ}{2}\ \ \mu^{1/3}}\right]\left[\frac{\mu}{\mu_{wall}}\right]^{1/4}\left[\frac{4\Gamma}{\mu}\right]^{1/9} \quad (19)$$

Assume $t_{wall} = 86°C \rightarrow \mu_{wal} = 0.002483\ ^{kg}/_{m.s}$
$\therefore h_\circ = 281.689\ \frac{w}{m^2\ K}$
The overall heat transfer coefficient Uo depend on the outside area of the tubes is

$$U_\circ = \left[\frac{D_\circ}{D_i\ \ h_i} + \frac{D_\circ}{D_i} * f_\circ + \frac{1}{h_\circ} + \frac{D_\circ}{2 * k} * \ln\frac{D_\circ}{D_i}\right]^{-1} \quad (20)$$

f: is the fouling factor for the hot waterequal 0.0002 m2*K/W [11]
k:the thermal conductivity of copper tubes. For copper tubes k=390 W/m°C
$\therefore\ U_\circ = 2.377\ \frac{w}{m^2 * °C}$
The logarithmic mean temperature difference LMTD is

$$LMTD = \frac{(t_{ws,e} - t_{hw,i}) - (t_{ss,i} - t_{hw,e})}{\ln\frac{(t_{ws,e} - t_{hw,i})}{(t_{ss,i} - t_{hw,e})}} \quad (21)$$

$\therefore$ LMTD = 11.2 °C
Q =A*U*LMTD $\rightarrow$ A = $\frac{Q}{U * LMTD}$ (22)
$\therefore$ A = 248.01 m^2
A = $\pi D_\circ L$ $\rightarrow L = \frac{A}{\pi\ D_\circ}$ $\rightarrow$ L = 2.4 m
Assume the safety factor is 1.15
L= 2.4 * 1.15 = 2.7 m
Assume the length of each tube turn is 0.3 m
n: number of turns

$$n = \frac{\text{total length of tube}}{\text{length of each tube}} = \frac{2.7}{0.3} = 9 \quad (23)$$

3.3 Calculation of Absorber Parameters

Shell and coil contribute to the absorber unit. The cooling water is inside the tube, and the solution is inside the shell. The mass balance and energy balance for the absorber are shown in Figure 3, and the conditions are listed in Table 3, and the fluid properties are listed in Table 4.

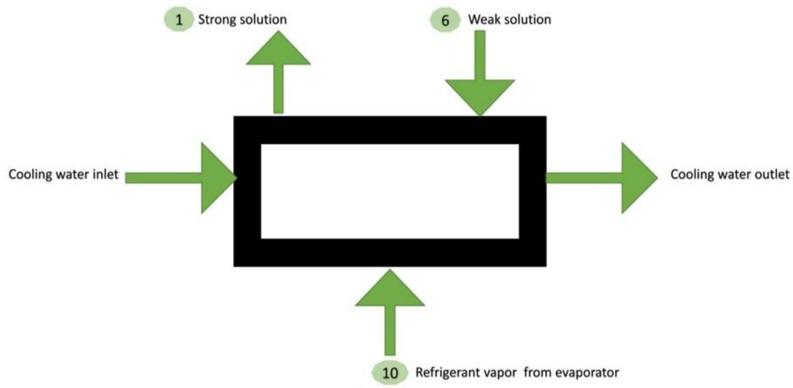

Figure 3:The mass balance and energy balance for Absorber

Table 3: Inlet and outlet data to the absorber

properties of cooling water at 35°C, P =5.6 kpa			Properties of LiBr at $\overline{T}$ =49°C And $\overline{X} = 59.7\%$		
ρ_w	994.08	kg/m^3	ρ	1694	kg/m^3
μ_w	0.0001016	$kg/m.s$	μ	0.004322	$kg/m.s$
k_w	0.01914	$w/m,c$	k	0.4299	$w/m.c$
Cp_w	1.924	$kJ/kg.k$	C_p	10916	$kJ/kg.k$
p_r	1.021		μ_{wall} at $t_{wall} = 36°C$	0.0045	$kg/m-s$

Table 4: the properties of cooling water and LiBr-water (Klein & Alvarado, 2004)

$\dot{Q}_a$	T_a	T_{ss}	X_{ss}	$\dot{m}_{ss}$	T_{ws}	X_{ws}	$\dot{m}_{ws}$	$T_{cw,i}$	$T_{cw,o}$	T_{av}
2.5	37	37	59	0.0150	61	60.7	0.0145	34	36	35
Kw	°C	°C	%	kg/s	°C	%	kg/s	°C	°C	°C

The mass flow rate of cooling water is:

$$\dot{m}_{cw} = \frac{\dot{Q}_a}{C_p\ \Delta t} = 0.649\ kg/s \tag{24}$$

The cooling water velocity in tube is:

$$V_{cw} = \frac{\dot{m}_{cw}}{\rho_w \frac{\pi}{4} D^2{}_i} = 4.2\ m/s \tag{25}$$

The Reynolds number of cooling water is:

$$Re = \frac{\rho_w * V_{cw} * D_i}{\mu} \rightarrow Re = 5753140.2 \tag{26}$$

The Nusselt number for fluids flowing inside the tubes:

$$Nu = 0.023\ (Re)^{0.8}\ (Pr)^{0.4} \tag{27}$$

$\therefore$ Nu = 5490 $\rightarrow$ Nu = $\frac{h_i\ \ D_i}{k}$ $\rightarrow$ $h_i = 8344.6\ \frac{w}{m^2\ \ °C}$

The outside heat transfer coefficient is evaluated from the following conditions:

For $\frac{4\Gamma}{\mu} < 2100$

$$\therefore\ h_\circ = \left[\frac{k^2\ \rho^{4/3}\ C_p\ g^{2/3}}{\frac{\pi\ d_\circ}{2}\ \mu^{1/3}}\right]^{1/3} * \left[\frac{\mu}{\mu_{wall}}\right]^{1/4} * \left[\frac{4\Gamma}{\mu}\right]^{1/9} \tag{28}$$

For $\frac{4\Gamma}{\mu} > 2100$

$$\therefore\ h_\circ = 0.01 * \left[\frac{k^2\ \rho^2\ g}{\mu^2}\right]^{1/3} * \left[\frac{\mu\ C_p}{k}\right]^{1/3} * \left[\frac{4\Gamma}{\mu}\right]^{1/3} \tag{29}$$

In this design:

$\Gamma = \frac{\dot{m}_{ss}}{2L_{tube}} = 0.0250\ \frac{kg}{m.s}$, and (30)

$\frac{4\Gamma}{\mu}$ =23.1 < 2100

Assume an average wall temperature is 36 °C

$\rightarrow\ \mu_{wall} = 4.5 * 10^{-3}\ \frac{kg}{m.s}$

$\therefore\ h_\circ = 4980.5\ \frac{w}{m^2\ °C}$

$U_\circ = 2.328\ \frac{w}{m^2 *\ °C}$

LMTD = 10.4 °C

Q = A * U∘ * LMTD (31)

A = π L d∘ → L = 2.9 m

Assume the safety factor is 1.15

$\therefore\ L = 2.9 * 1.15 = 3.3\ m$

∴ No. of turns (n) = 11

3.4 Calculation of Condenser Parameters

A shell and coil condenser type is selected. The refrigerant flows inside the shell, and cooling water flows in the tube. The mass and energy balance for the condenser is shown in Figure 4, and the conditions are listed in Table 5, and the fluid properties are listed in Table 6.

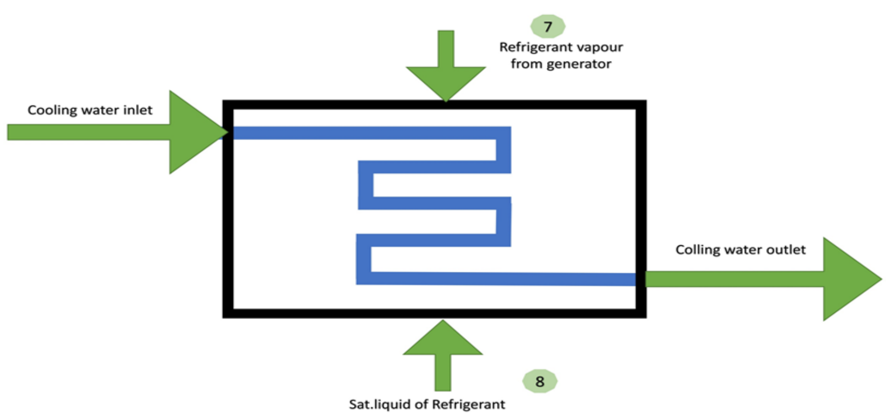

Figure 4: The mass and energy balance for condenser.

Table 5: Input and output data to the condenser

Q_c	T_c	m_r	$T_{cw,i}$	$T_{cw,e}$	$T_{cw)av}$
0.909	38	$4.253*10^{-4}$	30	34	32
kw	℃	kg/s	℃	℃	℃

Table 6:Properties of cooling water an refrigerant (Klein & Alvarado, 2004)

Properties of cooling water at 32.5℃			Properties of saturated refrigerant at 38 ℃, P = 6.6 kpa		
ρ_w	995	kg/m^3	ρ_l	933	kg/m^3
μ_w	0.000765	$kg/m.s$	μ	0.00001025	$kg/m.s$
k_w	0.06192	$w/m.c$	k	0.01936	$w/m.c$
p_r	5.161		h_{fg}	2411	KJ/Kg
			ρ_v	0.04608	kg/m^3

The mass flow rate of cooling water is:

$$\dot{m}_{cw} = \frac{\dot{Q}_c}{Cp_w \ \Delta t} = 0.869 \ kg/s \tag{32}$$

Inner diameter assumed is $(D_i) = 0.014$ m
Outer diameter assumed is $(D_\circ) = 0.016$ m
The velocity in tube is

$$V_{cw} = \frac{\dot{m}_{cw}}{\rho_w \ {}^{\pi}/_{4} \ {D_i}^2} = 5.7 \ m/s \tag{33}$$

The Reynolds number is

$$Re = \frac{\rho_w * V_w * D_i}{\mu_w} = 103791.2 \tag{34}$$

The flow is turbulent, Nussult number is

$$Nu = 0.023 \ Re^{0.8} * Pr^{0.4} \tag{35}$$

$\therefore Nu = 456.8$
The inside heat transfer coefficient is

$$h_i = \frac{Nu * k}{D_i} = 20203.6 \ \frac{W}{m^2 \ k} \tag{36}$$

The outer heat transfer coefficient two phase flow:

$$h_\circ = 0.725 * \left[\frac{\rho_l * g * h_{fg} * k^3 * (\rho_l - \rho_v)}{\mu * \Delta T * D_i}\right]^{\frac{1}{4}} \tag{37}$$

$\Delta T = T_c - T_{wall}$
Assume $T_{wall} = 36$ ℃
$\therefore \Delta T = 2$ ℃

$$\therefore h_\circ = 615.797 \ \frac{W}{m^2 \ ℃}$$

The fouling factor $f_\circ = 0.0002 \ \frac{m^2 \ .k}{w}$ [8]

$$U_\circ = \left[\frac{D_\circ}{D_i * h_i} + \frac{D_\circ}{D_i} * f_\circ + \frac{1}{h_\circ} + \frac{D_\circ}{2 * k} * \ln\frac{D_\circ}{D_i}\right]^{-1} \tag{38}$$

$$U_\circ = 2.399 \ \frac{W}{m^2 * ℃}$$

The log mean temperature difference is:

$$LMTD = \frac{(T_c - T_{cw,e}) - (T_c - T_{cw,i})}{Ln\frac{(T_c - T_{cw,e})}{(T_c - T_{cw,i})}} \quad (39)$$

LMTD = 5.77 °C

$$Q_c = U_\circ * A * LMTD \rightarrow A = \frac{Q_c}{LMTD * U_\circ} \quad (40)$$

$A_\circ = \pi * D_\circ * L \quad \rightarrow L = 1.6\ m$

Assume the safety factor is 1.15

L = 1.6 * 1.15 = 1.9 m

$\therefore$ No . of turns (n) = 6

3.5 Calculation of Evaporator Parameters

A shell and coil evaporator is chosen. The refrigerant flows inside the shell, and the chilled water is cooled in the coil. The mass and energy balance for the evaporator is shown in Figure 5, and the conditions are listed in Table 7, and the fluid properties are listed in Table 8.

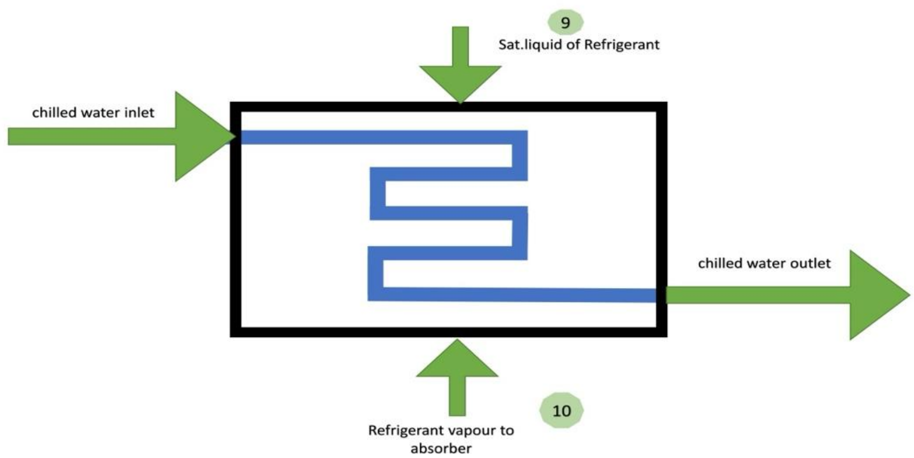

Figure 5: The mass balance and energy balance for Evaporator.

Table 7: Input and output data to the evaporator

Q_e	T_e	m_r	$T_{w,i}$	$T_{w,e}$	$T_{w)av}$
1	5	$4.253*10^{-4}$	12.5	7	9.75
Kw	°C	kg/s	°C	°C	°C

Table 8: Properties of chilled water and refrigerant (Klein & Alvarado, 2004)

Properties of chilled water at 9.75 °C, P=1.208 kpa			Properties of water refrigerant at 5 °C, P= 0.8725 kpa		
ρ	999.7	kg/m^3	ρ	1000	kg/m^3
K	0.5792	W/m. °C	K	0.01708	W/m. °C
μ	0.001315	kg/m. s	μ	$0.9336*10^{-5}$	kg/m. s
C_p	4.196	KJ/kg. k	C_p	1.889	KJ/kg. k
Pr	9.5		h_{fg}	2489	
			ρ_v	0.006802	kg/m^3

Assume Inner diameter = 0.014 m
Assume Outer diameter = 0.016 m
The mass flow rate of chilled water is

$$\dot{m}_{cw} = \frac{Q_E}{C_p \; * \; \Delta t} = \; 0.0433 \; kg/s \tag{41}$$

The water velocity in the tube is

$$V_w = \frac{\dot{m_w}}{\rho \quad A_i} = \frac{4\dot{m}}{\rho \; \pi \; {D_i}^2} \; = 0.282 \; m/s \tag{42}$$

Re = 3001.38 $\rightarrow$ the flow is turbulent
Nu = 27.35

$$h_i = \frac{Nu \; * k}{D_i} = 1131.5 \; \frac{W}{m^2 \; . \; ℃} \tag{43}$$

From the above the information the outer heat transfer coefficient two phase flow (Aljuhani & Dayem, 2022):

$$h_\circ = 0.725 * \; \left[\frac{\rho_l \; * g * \; h_{fg} * \; k^3 * (\, \rho_l - \; \rho_v)}{\mu * \; \Delta T * D_i}\right]^{\frac{1}{4}} \tag{44}$$

$$\therefore \; h_\circ = 474.71 \; \frac{W}{m^2 \; k}$$

$$U_\circ = 1.19 \; \frac{W}{m^2 \; ℃}$$

LMTD = 4.123 ℃

Q = A * LMTD * $U_\circ$ (45)

A = $\pi * \; d_\circ * L \quad \rightarrow \quad L = 1.1 \, m$

L = 1.1 * 1.15 = 1.5 m

$\therefore$ No. of turns (n) = 4

3.6 Heat Exchanger Design

Typically, a counterflow heat exchanger comprising two concentric copper tubes is employed for small-scale lithium bromide water cooling devices. In this section, a heat exchanger of that type is created with a hot weak solution in the outer pipe and a cold strong solution in the inner pipe. The conditions are listed in Table 9, and the fluid properties are listed in Table 10.

Table 9: Inlet and exit data to the heat exchanger

Q_{Hx}	$\dot{m}_{ss}$	$T_{ss,i}$	$T_{ss,e}$	$T_{ss,av}$	X_{ss}	m_{ws}	$T_{ws,i}$	$T_{ws,e}$	$T_{ws.av}$	X_{ws}
1.08	0.01501	37	57.9	47.5	59	0.0145	85	61	73	60.7
Kw	kg/s	℃	℃	℃	%	kg/s	℃	℃	℃	%

Table 10: the properties of LiBr solution (Klein & Alvarado, 2004)

properties of strong solution at $T_{av} = 47.5$ ℃, $X_{ss} = 59\%$			properties of weak solution at $T_{av} = 73℃, X_{ws} = 60.7\%$		
ρ	1683	kg/m^3	ρ	1704	kg/m^3
μ	0.004216	$kg/m.s$	μ	0.00319	$kg/m.s$
K	0.4314	$W/m.k$	k	0.44066	$W/m.k$
C_p	1.931	$KJ/kg.℃$	C_p	1.92	$KJ/kg.℃$

The following formula is used to find the heat exchanger's inside and outside heat transfer coefficients.

Assumed (5⁄8,1) is the outer and inner diameter.

$$Re = \frac{4\dot{m}_{ss}}{\pi\ \mu\ d_i} = 324.1 \tag{46}$$

The flow is laminar in strong solution → $Nu = 3.66$

$$\therefore\ h_i = \frac{Nu * k}{d_i} = 112.7\ \frac{W}{m^2.k}$$

the hydraulic diameter is:

$$D_h = D_\circ - D_i \ \rightarrow D_h = 0.0105\ m$$

$$Re = \frac{4 * m\dot{}_{ws}}{\pi * \mu * d_h} = 551.5$$

The flow is laminar in weak solution in heat exchanger

$\therefore Nu = 3.66$

$$h_\circ = 153.6\ \frac{W}{m^2\ k}$$

$$U_\circ = 2.377\ \frac{W}{m^2\ {}^\circ C}$$

$$Q_{hx} = LMTD * A * U_\circ$$

$A = \pi * D_\circ * L$

L = 0.1 m

3.7 Capillary Tube

In order to connect the evaporator inlet and condenser outlet of expansion device is required to lower the pressure and corresponding saturation temperature of refrigerant from the condenser condition to the evaporator condition The liquid refrigerant from the condenser passes through the capillary tube and expands as a result of the internal energy drop that occurs after the flash vaporization and the modification of other state characteristics (Sahoo & Das, 2014). In this investigation of water refrigerant, the design and computation of the capillary tube length employed a reference (Ameer, 2016). The predicted capillary tube length at the conclusion of the calculation process is 2.1 m.

3.8 Evacuating tube collector

In this project, the absorption chiller system's hot water requirements are met by means of the evacuated tube collectors. The installation of evacuated tube collectors in the location is justified by the temperature and radiation data of the area.

3.8.1 Features

High speed and high efficiency in heat transfer.

Low start-up temperature on heat energy and better resistance against lower temperatures, obvious advantages in performance in low temperatures and cold regions. The round structure automatically tracks the sunlight, maintains high efficiency throughout the day, with a stable heat supply. No water inside, no scale, which maintains efficient heat exchange for a long time. Pressurized type, independent design, the disassembly and assembly do not affect the system operation.

3.8.2 Specifications

The specifications of the solar collectors used are listed in Table 11 below.

Table 11: Specification of evacuated tube collectors

Modle	SFVB5818
Heat pipe (copper)	Specs: (14 +8) * 1800 Material: Red Copper Output Power >125w
Vacume tube	Specs: SFVB5818 Material:Borosilicate Glass 3.3 Absorber coating:Al/N/SS/CU Absorptivity >93% Reflectivity < 8%
Aluminum fin	5818
Silicone plug	58
Minimum temperature	- 35 ℃
Stagnation temperature of heat pipe bulb	222℃
Sun insolation power	>65W

4 Results and Discussion

Figure 6 shows the variation of pipe length for different components of the cycle (generator, absorber, condenser, evaporator) with the required cooling load for assumed design conditions.

Also, it can be seen from this figure that the length of coil pipe for all components is increased with increasing cooling load due to the increasing amount of heat that needs to be transferred with increasing system capacity, which requires extra surface area for the pipe to be able to transfer this amount of heat.

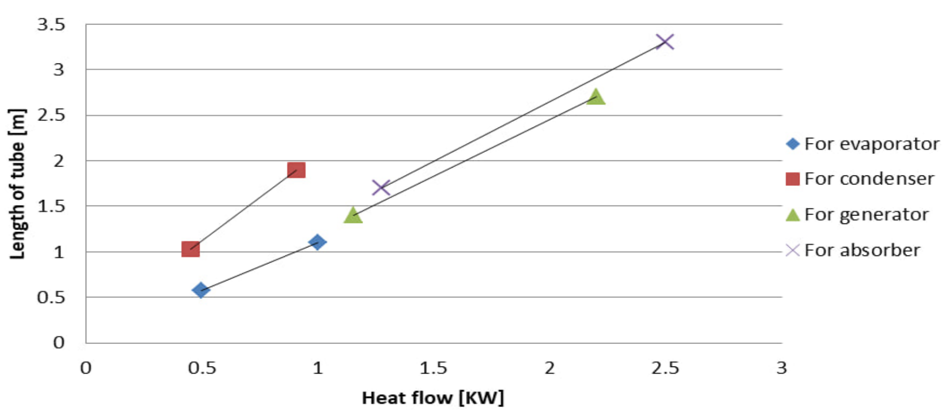

Figure 6:The variation between heat flow and length of tube

Figure 7 presents the variation between the number of tube turns with the cooling load required for the absorption refrigeration cycle parts (generator, absorber, condenser, evaporator) under the presumed design conditions. This figure shows that as the cooling load increases, the number of turns for every component increases, due to increasing the tube length as shown in Figure 6.

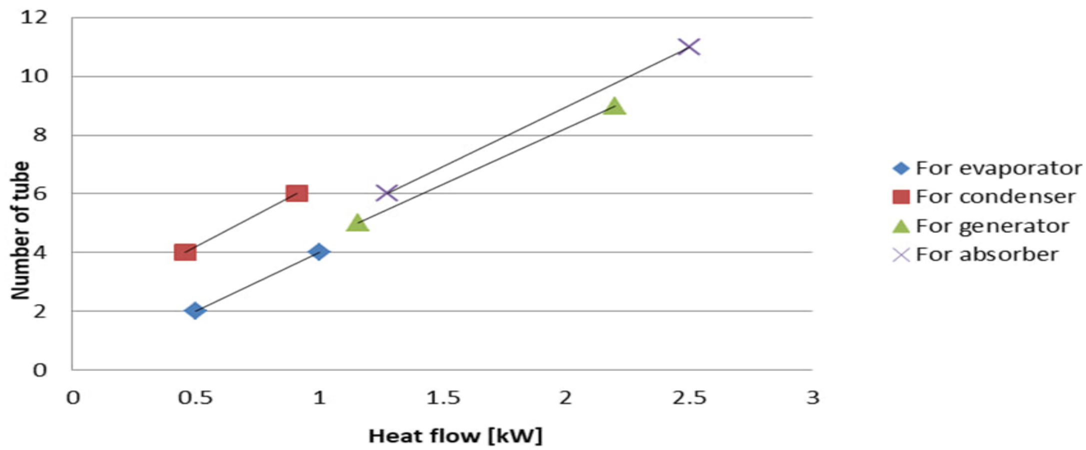

Figure 7: shows the variation of number of tube with cooling load

5 Conclusion

We have presented a design of a single-effect, fully solar-powered hot water absorption chiller with a cooling capacity of 1 kW to achieve high energy efficiency and reduce greenhouse gas emissions in buildings using lithium bromide and water as a working pair because lithium bromide and water solutions exhibit favorable thermodynamic properties for absorption cooling. The vapor pressure of the solution is much lower than that of pure water at the same temperature, allowing for efficient absorption of water vapor (refrigerant) at low pressures. Compared to some other working fluids, aqueous solutions containing lithium bromide are relatively non-toxic and safe to handle, reducing safety concerns during operation and maintenance. In this design, the solar radiation of the city of Nasiriyah in southern Iraq was relied upon to produce hot water for a cooling generator. It was designed to cool a room made of sandwich panels with dimensions of 1 × 1 × 1.80, and the assumed generator temperature was 85 °C, the hot water temperature coming from the solar collector was 90 °C, and the required cooling temperature was 7 °C. The results showed that the design is reliable and applicable to any cooling load and that as the cooling load increases, the tube length and number of coils increase.

6 References

Aljuhani, Y., & Dayem, A. M. A. (2022). Thermal analysis of a solar-powered absorption air-conditioning system: Case study for a tent in Mina zone, Saudi Arabia. *Cleaner Engineering and Technology*, *8*, 100472. https://doi.org/10.1016/j.clet.2022.100472

Ameer, A. S. (2016). Experimental and Theoretical Study of Absorption Cooling System Integrated with Solar Concentrated Collector. *PhD Dissertation*.

Ataa, A. B., & Ammarib, H. (n.d.). *Simulation of a LiBr-Water Absorption Refrigeration System Powered by Evacuated Tubes Solar Collector*.

Dalichaouch, M. (1989). *A theoretical and experimental investigation of an absorption refrigeration system for application with solar energy units*. Newcastle University.

Eicker, U., & Pietruschka, D. (2009). Design and performance of solar powered absorption cooling systems in office buildings. *Energy and Buildings*, *41*(1), 81–91. https://doi.org/10.1016/j.enbuild.2008.07.015

Ketfi, O., Merzouk, M., Merzouk, N. K., & Metenani, S. El. (2015). Performance of a Single Effect Solar Absorption Cooling System (Libr-H2O). *Energy Procedia*, *74*, 130–138. https://doi.org/10.1016/j.egypro.2015.07.534

Klein, S. A., & Alvarado, F. L. (2004). Engineering Equation Solver (EES) Software. *Department of Mechanical Engineering, University of Wisconsin—Madison*.

Narayanan, R., Harilal, G. K., & Golder, S. (2021). Feasibility study on the solar absorption cooling system for a residential complex in the Australian subtropical region. *Case Studies in Thermal Engineering*, *27*, 101202. https://doi.org/10.1016/j.csite.2021.101202

Osman, E. A., & Abdalla, K. N. (2016). Design and Construction of an Absorption Cooling System Driven by Solar Energy. *University Of Khartoum Engineering Journal*, *6*(ENGINEERING).

Sahoo, K. C., & Das, S. N. (2014). Theoretical design of adiabatic capillary tube of a domestic refrigerator using refrigerant R-600a. *American Journal of Engineering Research*, *3*(05), 306–314.

William, B. J., Selvaraj, A., Rammurthy, M. S., Rajaraman, M., & Srinivasa Chandra, V. (2017, March 28). *A Study on Implementation of Vapour Absorption Air Conditioning System (VAAcS) Using LiBr-H 2 O in Commercial vehicles*. https://doi.org/10.4271/2017-01-0181